Environmental Science Advances

ROYAL SOCIETY OF CHEMISTRY

PAPER

View Article Online
View Journal | View Issue

Cite this: *Environ. Sci.: Adv.*, 2023, **2**, 1540

The association of air quality and complex atmospheric oxidation chemistry in the dispersion and deposition of SARS-CoV-2-laden aerosols

Sandhiya Lakshmanan, *[a] Ranjana Aggarwal, [a] Kittusamy Senthilkumar [b] and Anupama Upadhayay[a]

The present study investigates the effects of air pollution and climate factors on the acceleration of SARS-CoV-2 transmission and mortality. In particular, the correlations between O_3, NO_2, $PM_{2.5}$, PM_{10} and SO_2 concentrations with daily number of infections and fatalities caused by the second wave of COVID-19 during the time period March–June 2021 in Indian cities with different climate zones are analyzed. The chemical transformations in the atmosphere that translated to dispersion of SARS-CoV-2 aerosols and their deposition in the respiratory system are studied. The results suggested that exposure to a higher level of O_3 may weaken the respiratory system, and therefore resistance against COVID-19 is suppressed. The infectious aerosols undergo reactive encounters with atmospheric oxidants, forming secondary aerosols before deposition in the lungs. The pulmonary epithelium is naturally protected against atmospheric O_3 and secondary aerosols by lung-lining fluids that contain ascorbic acid, AH_2 and other antioxidants. Since O_3 and COVID-19 infections showed a positive correlation, AH_2 and the underlying tissues will be the most affected. The mechanism for the interaction of O_3 with AH_2 is studied using quantum chemical methods. During this interaction, a persistent ozonide is formed in lung-lining fluids and this is acidified by the inhaled aerosols. Earlier epidemiological and toxicological studies revealed that this ozonide leads to the formation of cytotoxic free radicals that can cause oxidative stress during breathing. Thus, O_3 plays a significant role in the deposition of aerosols in the lungs. The results of this study add to prevailing evidence as well as providing new insights into the role of ambient O_3 in the dispersion and deposition of SARS-CoV-2 aerosols.

Received 24th January 2023
Accepted 8th September 2023

DOI: 10.1039/d3va00016h

rsc.li/esadvances

Environmental significance

Aerosol spreading of coronavirus SARS-CoV-2 is identified as one of the significant pathways for transmission of COVID-19. This airborne transmission through aerosols is largely associated with air pollution and meteorological factors for the dispersion of infectious aerosols and their consequent deposition on surfaces and the respiratory tract. Our study reveals the correlation between daily average O_3 concentration and relative humidity (RH) in the spread of COVID-19 infections. The relative humidity has control over the ozone production and deposition and modulates the transmission of ozone-containing droplets. The study establishes the possible role of ground-level ozone on the dispersion and deposition of SARS-CoV-2 aerosols.

1. Introduction

Coronavirus disease 2019 (COVID-19) emerged as an epidemic and then evolved into a pandemic,[1] and led to great disruption by destroying the lives and livelihoods of several million people all around the globe. COVID-19 is caused by infection with severe acute respiratory syndrome coronavirus 2 (SARS-CoV-2). Extensive research on the coronavirus SARS-CoV-2 shows that the major transmission pathway for COVID-19 is through aerosols[2] and the virus remains airborne for several hours and on surfaces up to days.[3–5] This airborne transmission is extremely infectious and is the central route for spreading COVID-19.[6] This transmission is caused by the inhalation of small droplets or respiratory droplets containing SARS-CoV-2 that are produced during expiratory events such as breathing, speaking, sneezing, or coughing.[7–10] These virion droplets with a broad size range from <0.8 to 10 μm[11,12] also contain salts and other biomolecules. On exposure to ambient air these small droplets interact strongly with particulate matter (PM) and remain suspended in the air as aerosols for several hours. Larger droplets with size > 5 μm will quickly be deposited on the ground due to gravity and transmit the virus over relatively short distances, whereas the smaller droplets are efficiently dispersed

[a]CSIR – National Institute of Science Communication and Policy Research, New Delhi 110012, India. E-mail: sandhiya@niscpr.res.in
[b]Department of Physics, Bharathiar University, Coimbatore 641046, Tamil Nadu, India

in the air thereby possessing a longer lifetime in air, so they can transfer the virus over longer distances.[13,14] However, as reported earlier,[62] exhaled particles which have a diameter of 5–10 μm under the influence of gravity will fall slowly to the ground and they are too small to settle on the ground further than 1–2 m from the source. Exhaled particles larger than 50–100 μm, which are produced during sneezing or coughing, can be carried beyond 1–2 m. The volume of aerosols generated by sneezing, coughing, talking and breathing by an individual are estimated at 1000 nL, 100 nL, 10 nL min^{-1} and 1 nL min^{-1}, respectively[15] The viral load of SARS-CoV-2 in saliva is 1000 virions per nL[15] and hence a COVID-19 patient could produce at least 1000 airborne SAR-CoV-2 virions per minute.[16] The concentration of virions is continuously diluted during aerosol transmission from an infected individual to the host before deposition in the human respiratory tract.[17] Hence, the airborne transmission of SARS-CoV-2 is likely to occur in indoor environments with poor ventilation and for individuals with continued contact with medical procedures that generate aerosols.[16]

Despite existing evidence, the airborne transmission of SARS-CoV-2 is still inconclusive. This is partly attributed to the unclear understanding of the relative roles of droplets and aerosols during virus transmission. The binding of virus particles with the aerosols depends upon the atmospheric conditions and they remain floating in the air for a longer time than isolated droplets.[16] Hence, a deeper understanding of the atmospheric fate of these droplets through physical and chemical processes leading to aerosol dispersion and deposition is essential. Physical parameters such as air temperature and relative humidity strongly influence the survival of the virions in air and their dispersion.[18] Modelling studies show that during coughing and sneezing, the droplets are radiated in turbulent gas clouds and hence the physical parameters of the cloud have an impact on the evaporation dynamics of the aerosols.[14,19] For instance, the relative humidity (RH) of the cloud has greater potential to stimulate the infectivity of the virus before it is dispersed in air.[20] Hence, the RH in cloud which is higher than ~85% has stronger implications for virus spread with longer lifetime aerosols than the RH in interior spaces, which is ~40%.[20] Furthermore, the droplets emitted from the body during coughing and sneezing will be warmer than the ambient temperature, where the larger droplets suffer little or no effect from the surrounding cloud and the smaller droplets tend to move along the cloud and travel over long distances.[19] Hence, RH and air temperature are the important physical factors in dispersing the virions in air.

Air pollution is considered one of the threat factors in spreading COVID-19, where an increase in 8% COVID-19 death rate is observed with an increase of 1 μg m^{-3} of particulate matter.[21–23] The respiratory system is the part most affected by SARS-CoV-2 and the inhaled aerosols deposit in different regions of the respiratory system. Upon exposure to air pollutants, such as ozone (O_3) and nitrogen dioxide (NO_2), free radicals are produced through heterogeneous and multiphase chemistry on reactive encounters between different air pollutants and atmospheric oxidants. The free radicals can damage the respiratory and immune systems by modifying a host which is resistant towards viral and bacterial infections.[24] The inhaled aerosols with size larger > 5 μm will be deposited in the upper regions of the respiratory tract and will be removed most commonly by being spat out.[25] But the smaller aerosols inhaled penetrate to the alveolar region of the lung, where the primary removal mechanism is by pulmonary surfactant proteins which are lung-lining fluids.[26] The atmospheric pollutants O_3 and NO_2 can react with the lung-lining fluids, resulting in the nitration of surfactant proteins. The nitrated protein conjugates evade immune tolerance and boost immune responses and therefore enhance respiratory and allergic diseases.[27,28] This shows that nitration of surfactant proteins is one of the important biochemical processes occurring during deposition and inhalation of aerosols. Therefore, correlating the relationship between O_3 and NO_2 concentrations in the atmosphere and SARS-CoV-2 infections will provide further insight into the impact of air quality on the spread of COVID-19.

Understanding the spread of COVID-19 and the ways to control it are priority areas of investigation, as when the second wave of COVID-19 occurred, India became the worst-hit victim of this second wave. This second wave was due to the circulation of various double-mutant and triple-mutant strains of SARS-CoV-2 across different regions of India, where the mutant strains were more pathogenic than the initial strains.[29] There are several reasons behind the massive surge and increasing number of deaths in the second wave of COVID-19 in India. One reason could be the poor air quality index of India which hinders the Indian population in combatting COVID-19, since there is a high possibility that the respiratory system is already affected by air pollution. In view of the existing evidence that climate factors such as air temperature and humidity (responsible for the dispersion of aerosols) and biochemical processes involving aerosols and air pollutants (responsible for deposition in the lungs) as influential factors for SARS-CoV-2 infections and spread, the goal of the current study is to correlate the relationship between these factors with real-time data of COVID-19 infections and fatalities. The transmission pathway of SARS-CoV-2 from aerosol dispersion in air to deposition of aerosols in the lungs will be analyzed from these factors. As Delhi in India is one of the most polluted cities and is also the city most affected by the spread of COVID-19 infections and mortality, this study examines the effect of air pollution and climate factors in the spread of SARS-CoV-2 in Delhi. Three other cities in different climate zones affected by COVID-19 in different periods of time are also investigated to understand the impact of air pollutants in the dispersion of SARS-CoV-2 aerosols.

2. Materials and methods

2.1 Sites under study

Three cities (Delhi, Pune, and Trivandrum) and one state (Assam) in India in different climate zones were chosen for the study. Delhi, the capital city of India with 13.8 million inhabitants, is a highly industrialized region of the country and is a significant spot for air pollution. For the past several years,

the ambient air quality data in Delhi has shown very high values of O_3, NO_2 and eventually $PM_{2.5}$ beyond permissible limits, especially during winter. The major factors for the increasing levels of air pollution in Delhi are attributed to the city's landlocked geographical location, stubble burning from neighboring states, and emissions from vehicles, industries and construction sites. Despite the lockdown restrictions and several precautionary measures, Delhi was one of the most affected cities in the second wave, where the daily new cases increased rapidly from ~400 in mid-March 2021 to ~27 000 cases at the end of April 2021. Complete lockdown was imposed in Delhi from 17 April 2021 to 31 May 2021 and this effort led to a substantial decrease in the number of COVID-19 infections, bringing the number down to ~600 at the end of May 2021. Pune, located in the western part of India is at a higher altitude and is on the leeward side of the Sahyadri range of mountains with a population of 5 million. The city was badly affected by both waves of COVID-19. Despite severe restrictions, the daily numbers of cases increased from ~1900 on 16 March 2021 to ~4000 on 2 May 2021. The curve got flattened after 17 June 2021. A recent study[30] reported that the average ozone concentration showed a marginal increase during the lockdown period of the first wave of COVID-19, revealing the impact of ozone concentration on the spread of COVID-19. Trivandrum, situated on the southwest coast of India is characterized by fairly flat terrain with relatively less industrial activity. In this tropical site, in contrast to high-altitude locations, meteorology plays a significant role in long-term surface ozone concentration.[31] The daily number of COVID-19 cases in Trivandrum increased rapidly from ~100 to ~4500 from 16 March to 14 May 2021. The number of cases decreased gradually after 14 May, but was still ~1500 at the end of June 2021. Assam, the state in Eastern India located in the Brahmaputra Valley region is different from the other parts of India due to the influence of the Ganga Basin and the Bay of Bengal. Though the region is moderately polluted and populated, the average O_3 concentration in Guwahati, Assam is relatively low compared with other urban sites in India.[32] COVID-19 infections hit Assam only in mid-April 2021 and the number was ~2500 at the end of June 2021. Owing to the variations in ozone concentration, meteorology and daily number of COVID-19-positive cases, the four sites mentioned above were chosen for the study. Depending on these data, in the case of Delhi, the period chosen for analysis is 16 March 2021 to 31 May 2021 and in the other three cases, the period of study is from 16 March 2021 to 30 June 2021.

2.2 Data used and method of analysis

Daily average ambient concentrations of O_3, NO_2, $PM_{2.5}$, PM_{10} and SO_2 for Delhi, Pune, Assam and Trivandrum were obtained from the Central Pollution Control Board (CPCB), Government of India. Meteorological parameters, such as relative humidity (RH), wind intensity, temperature and precipitation rate, for Delhi were retrieved from the IARI Meteorological Database System, New Delhi. The data for COVID-19 infections and fatalities were obtained from the data repository by the Center for Systems Science and Engineering (CSSE) at Johns Hopkins University, which aggregated the data from the Government of India (**https://www.mygov.in/covid-19**). The relationship between air pollution factors and meteorological variables with COVID-19 infections and fatalities were assessed through Pearson correlation tests and represented as correlograms. Where necessary, the Spearman correlation coefficient was used and compared with the Pearson correlation coefficient. Furthermore, the data used in the current study are not normally distributed and hence correlation tests are used as empirical methods for determining the relationship between air pollution, climate factors and COVID-19 infections. ORIGIN 10 software was used for this analysis and Rstudio was used to prepare the correlograms.

2.3 Quantum chemical methodology

Density functional theory (DFT) calculations at M06-2X/6-311++G(d,p) level of theory were performed to study the interaction of O_3 with the lung-lining fluid ascorbic acid (AH_2). M06-2X is a meta-hybrid exchange–correlation functional which has been proved to provide the best description of hydrogen-bonding interactions, thermochemistry and chemical kinetics.[33] The stationary points on the ground-state potential energy surface (PES) of the reaction between AH_2 and O_3 in the gas phase were optimized at M06-2X/6-311++G(d,p) level. The solvent-phase calculations were performed by optimization at M06-2X/6-311++G(d,p) level in combination with the PCM model. In order to mimic lipid and aqueous environments within the lung-lining fluids, pentylethanoate and water were used as respective solvents, with dielectric constants of 4.73 and 78.35. Harmonic vibrational frequency analysis at the same level revealed the nature of the stationary points. All minima were confirmed with all positive frequencies and each transition state had one imaginary frequency. Intrinsic Reaction Coordinate (IRC) calculations were performed to determine the connectivity of the transition state with the designated reactants and products. The reaction of O_3 and AH_2 on the air–water interface was modelled by considering a water cluster with 10 water molecules and an additional OH^- ion. Thus, the model system considered here will be able to provide a reasonable description of the interfacial chemistry occurring at the air–water interface. All the electronic structure calculations were performed using the Gaussian 09 program.[34]

3. Results and discussion

3.1 Air pollution factors

The association of air pollutants such as O_3, NO_2, $PM_{2.5}$, PM_{10} and SO_2 with COVID-19 fatalities and infections in three Indian cities, Delhi, Pune, Trivandrum, and one state Assam in different geographic and climatic zones was analyzed. The variations in average pollutant concentrations in relation to daily fresh COVID-19 cases and daily deaths for the analyzed period are shown in Fig. 1.

In Delhi, a huge spike in the daily number of fresh cases was observed from 17 to 30 April 2021, where the average daily $PM_{2.5}$,

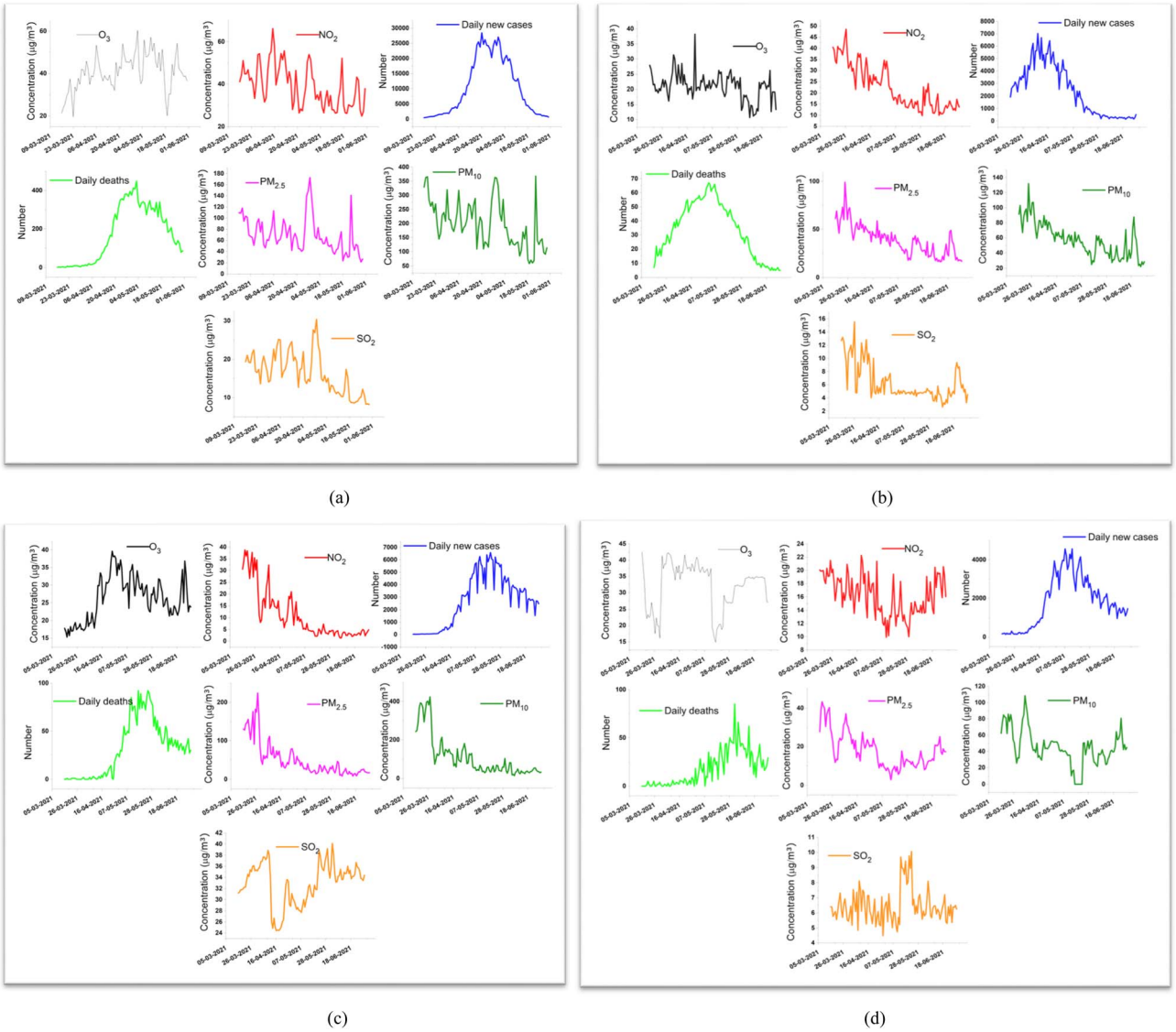

Fig. 1 Variation in daily averaged pollutant concentrations in (a) Delhi, (b) Pune, (c) Assam and (d) Trivandrum for the studied time period with COVID-19 cases and fatalities.

NO_2, PM_{10}, O_3 and SO_2 concentrations for this period were 86.1 ± 46.5, 38.4 ± 9.5, 219.2 ± 96.6, 45.98 ± 6.36 and 19.7 ± 5.7 μg m^{-3}, respectively. Prior to this period, the respective averaged concentrations were 79.0 ± 20.3, 46.3 ± 11.3, 240.8 ± 57.2, 36.34 ± 7.2 and 19.5 ± 3.2 μg m^{-3}, and for the month of May, the $PM_{2.5}$, NO_2, PM_{10}, O_3 and SO_2 concentrations were 60.0 ± 22.9, 32.3 ± 6.0, 142.4 ± 67.4, 43.21 ± 9.07 and 11.4 ± 2.5 μg m^{-3}, respectively. The pollutant concentrations exceeded the National Ambient Air Quality Standards (NAAQS). During the peak and pre-peak COVID-19 period, the $PM_{2.5}$, NO_2, PM_{10} and O_3 concentrations were at their peak and decreased gradually in the period after 30 April 2021, when COVID-19 cases started to decline. This shows that the O_3 concentration was higher during the period when COVID-19 cases were at their peak. This is also associated with fatalities due to COVID-19 in this period. The decrease in the pollutant concentrations in May 2021 is due to the impact of lockdown in Delhi enforced from 17 April 2021 to 31 May 2021. Average concentrations of $PM_{2.5}$, NO_2, PM_{10}, O_3 and SO_2 reduced by about −43.5%, −18%, −53.9%, −6.4%, and −72.8%, respectively, in May 2021 compared to the pre-lockdown period (16 March to 16 April 2021). A similar reduction in $PM_{2.5}$ and PM_{10} concentrations was observed in the lockdown period of March 2020 in Delhi.[35] In the case of O_3 and NO_2, the reduction is very low compared to the other pollutants. This may be attributed to the fact that in the Indian sub-continent, O_3 concentrations are at their peak during the period April to August.[36] Although during the study period there was an increase and decrease in O_3 concentrations, the net production of O_3 was not affected during this period. The enhancement in O_3 concentration during the lockdown period is due to the rather weak negative effect of photophysical processes. Thus, O_3 is not the only pollutant that enhances the spread of COVID-19 infections, but there are other individual atmospheric processes that may play a role. Thus,

there were fewer infections on some days, even when the O_3 concentrations were high.

In Pune, the peak in the daily new cases was observed during the period 31 March 2021 to 8 May 2021. During this period, the average $PM_{2.5}$, PM_{10}, O_3, NO_2 and SO_2 concentration levels were 39.4 ± 10.1, 57.2 ± 14.6, 22.52 ± 4.18, 27.21 ± 5.72 and 5.9 ± 2.2 μg m^{-3}, respectively. Prior to this period, running from 16 March 2021 to 30 March 2021, the respective concentrations were 65.1 ± 13.2, 92.9 ± 16.0, 21.9 ± 2.6, 38.5 ± 4.6 and 10.3 ± 3.2 μg m^{-3}. The O_3 concentrations were almost the same as those in the COVID-19 peak period, while the concentration levels of other pollutants were higher than those of the COVID-19 peak period. Although the daily new cases showed a rapid decrease after 8 May 2021, the fatalities showed a surge from 20 April 2021 to 20 May 2021, while the respective O_3 and NO_2 concentration levels were the same during this period.

The daily cases surged during the period 8 May to 19 June 2021 in the case of Assam. As shown in Fig. 1, during this period, the average $PM_{2.5}$, PM_{10} and NO_2 concentrations decreased rapidly as an impact of lockdown, whereas the average O_3 and SO_2 concentrations peaked at 27.2 ± 3.93 and 34.0 ± 2.9 μg m^{-3}. The major sectors contributing to air pollution in Assam are refineries and vehicle exhausts. Even in the absence of vehicles and with refineries functioning at lower capacities, the O_3 and SO_2 pollution levels increased during the lockdown period. In the case of Trivandrum, as noted from Fig. 1, during the peak COVID-19 period, there was an elevated level of O_3 concentration and reduced levels of $PM_{2.5}$, PM_{10}, and NO_2 concentrations. This observation is again suggestive of the fact that in most of the regions studied, atmospheric O_3 concentrations were increasing during the peak COVID-19 period.

The relationship between air pollutants and COVID-19 daily new cases and fatalities was studied through correlation

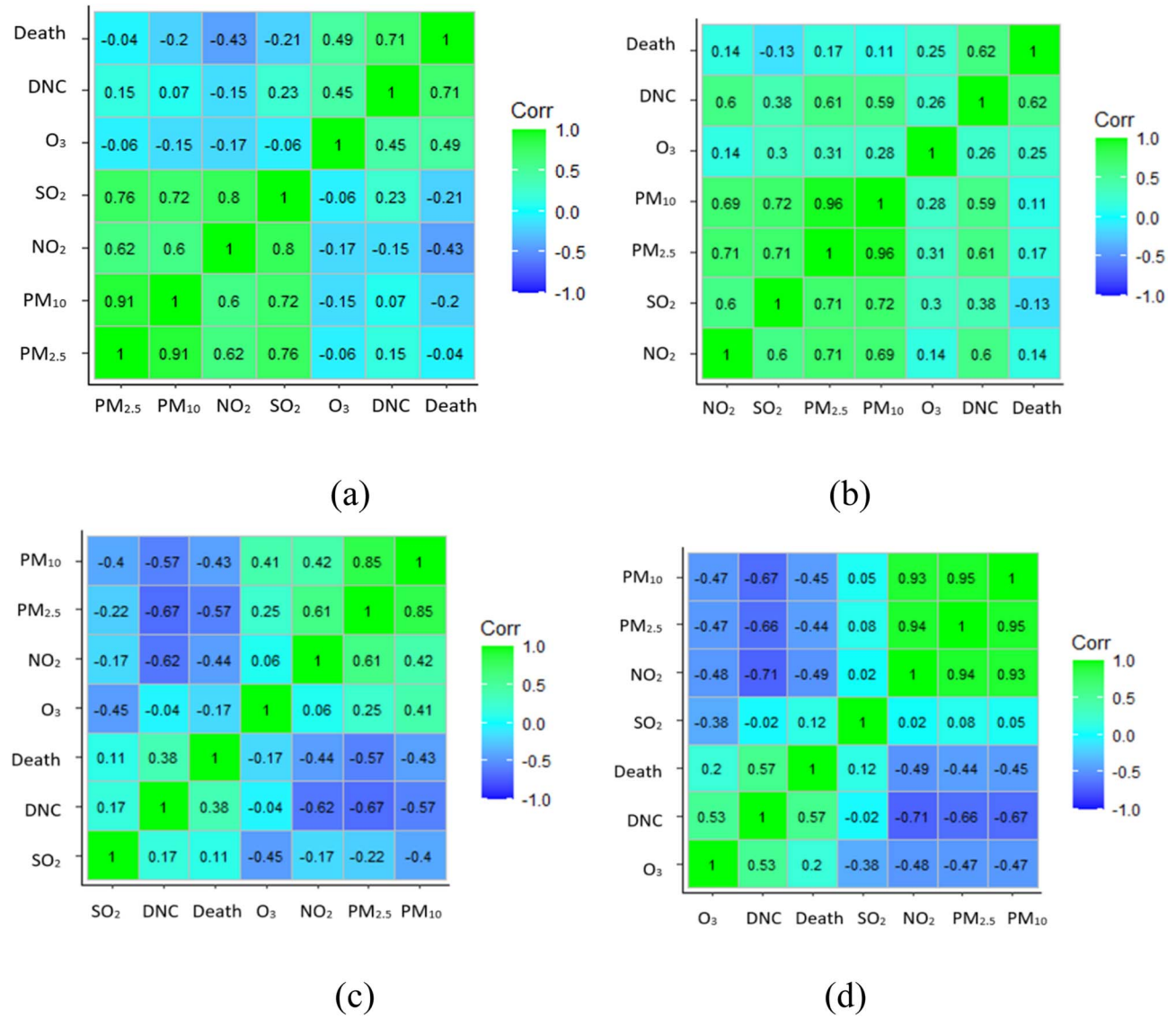

Fig. 2 Correlation between daily new cases (DNC), deaths and atmospheric O_3, NO_2, $PM_{2.5}$, PM_{10} and SO_2 concentrations for the studied time period in (a) Delhi, (b) Pune, (c) Trivandrum and (d) Assam.

analysis. The correlation between the concentrations of air pollutants and COVID-19 cases and mortality is represented as a correlogram for each of the four regions studied and they are shown in Fig. 2. In Delhi, the O_3 concentration levels and the daily new cases and deaths are positively correlated and the correlation is strong compared to the other pollutant concentrations. The NO_2 concentrations are negatively correlated with COVID-19 fatalities. Among the pollutants, the correlation between PM_{10} and $PM_{2.5}$ is strong with $R^2 = 0.91$, followed by a strong correlation between SO_2 and NO_2 and between $PM_{2.5}$ and SO_2. The NO_2 concentration levels strongly correlate with $PM_{2.5}$ and PM_{10} levels with $R^2 = 0.62$ and 0.60, respectively. The correlation of O_3 with other pollutant concentrations is very weak.

In the Pune region, the correlation between $PM_{2.5}$, NO_2 and PM_{10} and daily new COVID-19 cases is strong with Pearson coefficients of 0.61, 0.60 and 0.59, respectively. This tendency is followed by SO_2 showing a moderate correlation and, unlike the Delhi region, O_3 and daily new cases show weak correlation with $R^2 = 0.26$. In the case of correlation among pollutant concentrations, the same trend as observed in the Delhi region is followed in the Pune region. The $PM_{2.5}$, NO_2 and PM_{10} concentrations are strongly negatively correlated with the daily new cases as well as the mortalities. The SO_2 and the O_3 concentration levels show very weak correlation with COVID-19 fatalities. In contrast to Delhi and Pune, the SO_2 and O_3 concentrations are strongly negatively correlated, whereas the correlations among the other pollutants remain the same. In the case of Assam, the NO_2, $PM_{2.5}$ and PM_{10} levels are strongly negatively correlated with the daily cases with $R^2 = -0.71$, -0.67 and -0.66, respectively, and the O_3 levels are strongly positively correlated with the daily cases showing $R^2 = 0.53$. The relationship among the pollutant concentrations in Assam reveals that $PM_{2.5}$ and PM_{10} show perfect positive correlation with Pearson coefficient of 0.95 and this is followed by $PM_{2.5}$ and NO_2, and PM_{10} and NO_2 with R^2 values of 0.92 and 0.93, respectively. NO_2 and O_3 show a strong negative correlation of $R^2 = -0.48$.

The correlation analysis implies that, except for the Delhi region, the $PM_{2.5}$, NO_2 and PM_{10} concentrations are strongly positively correlated with the COVID-19 cases in Pune and the respective correlations are negative in Assam and Trivandrum. The correlation analysis reveals that the fatalities and infections due to COVID-19 with respect to air quality are not the same in all the regions studied. This indicates that the atmospheric oxidation chemistry is complex and depends upon several factors, determining the influence of air quality on the COVID-19 infections and fatalities in each of the cities. For instance, in the Delhi region, the O_3 levels show a strong correlation with the COVID-19 fatalities and all the other pollutant levels show very weak correlations. This is also due to the increase in O_3 concentration levels in Delhi when compared to the PM concentrations during the study period. The daily averaged O_3 concentration levels and air temperature show a positive correlation with $R^2 = 0.74$, revealing that the photolysis rate of O_3 production is enhanced through the following reactions:[37]

$$NO_2 + h\nu \rightarrow NO + O\ (\lambda < 420\ \text{nm}) \quad \text{(R1)}$$

$$O + O_2 + M \rightarrow O_3 + M \quad \text{(R2)}$$

$$O_3 + NO \rightarrow O_2 + NO_2 \quad \text{(R3)}$$

$$O_3 + h\nu \rightarrow O_2 + O(^1D)\ (\lambda < 320\ \text{nm}) \quad \text{(R4)}$$

The air temperature controls the solar radiation and the associated changes in solar radiation affect the above-mentioned photochemical oxidation reactions. As the solar radiation increases and in a NO_x-rich environment, the production of ozone is enhanced (R1) and (R2) and in conditions where NO_x is limited and solar radiation increases, destruction of ozone takes place (R4). The presence of aerosol in the atmosphere interferes with solar radiation and agitates the photochemical oxidant cycle and modifies ozone production. Thus, during the lockdown period, even with significant reductions in NO_2 emission levels, O_3 concentration levels increased and this led to the formation of secondary organic aerosols (SOAs) and particulate matter. The fog or cloud within SOAs creates a surface surrounding the gas, enhancing surface-mediated chemical reactions and there is also a bulk condensed phase where electron-transfer, acid–base and hydrolysis reactions occur. Thus, the airborne particles provide a condensed surface that represents a reactive surface with the atmosphere in addition to natural ground such as soil, ice, and snow.[38] Such aerosol–cloud interactions are influenced by the RH and as the SARS-CoV-2-laden aerosol may be composed of mostly sulfate and nitrate, which are hydrophilic, any change in RH can lead to a change in the size distribution and composition of the aerosols. Delhi's O_3 concentration levels for the period of analysis show a positive correlation with RH. This again leads to the photolysis of NO_2, eventually forming O_3, and the RH effect on photolysis will be proportional to the effect of aerosol loading. Thus, the ground-level ozone concentration depends on NO_x emission levels, RH and PM aerosol loading, which are coupled in the photochemical oxidation cycle. Thus, the increase in NO_2, $PM_{2.5}$ and PM_{10} levels also has a tendency to increase O_3 concentration levels. Owing to the correlation between air pollutants and COVID-19 cases and fatalities, and the significance of NO_2, $PM_{2.5}$ and PM_{10} levels in ozone chemistry, the impact of O_3 and NO_2 on COVID-19 cases is very relevant and is discussed below in detail.

The SOA formed from the dispersion of aerosols and atmospheric oxidation of O_3 has several impacts on health, in particular leading to respiratory diseases by deposition on the lungs. Hence, it is essential to understand the correlation between atmospheric O_3 concentration levels and COVID-19 cases and fatalities. In the case of Delhi, during the pre-lockdown period (16 March to 16 April 2021), the NO_2 concentration levels were higher than the O_3 concentration levels and during the complete lockdown period (17 April to 31 May 2021), O_3 concentration levels were higher than NO_2 concentration levels. The O_3 concentration levels in the lockdown period (17 April to 31 May 2021) increased by 20.4% compared to the pre-lockdown period (16 March to 16 April 2021), whereas the NO_2

concentration levels decreased by 25.9%. The NO_2 concentration levels showed a negative correlation with the O_3 levels with $R^2 = -0.17$. The increase in O_3 concentration levels is correlated with the reduction in NO_x emission levels which is in agreement with recent reports for COVID-19-hit cities such as Milan in Italy[39] and Wuhan in China.[40] In contrast to Delhi, the concentrations of O_3 and NO_2 are positively correlated in Pune with $R^2 = 0.31$. This shows that, aside from NO_2 which is involved in the destruction of ozone, other volatile organic compounds (VOCs) are emitted which are also precursors for ground-level ozone. In the case of Assam, the concentration of O_3 was at its peak during the lockdown period, and the daily average NO_2 concentrations were negatively correlated with those of O_3 levels with $R^2 = -0.48$. Except for a very few days, the O_3 concentration levels in Trivandrum were about twice as high as those of the NO_2.

3.2 Complex chemical phenomena of air pollutants

As discussed in the previous section, the lockdown periods in the COVID-19 pandemic improved the air quality by reducing the emissions of critical pollutants. Few pollutants are emitted directly as primary pollutants and the oxidation process in the atmosphere leads to secondary pollutants. The emissions of NO_2 and SO_2 are direct, whereas the other pollutants are formed through atmospheric chemical reactions. In the studied regions, NO_2 emissions showed a considerable decline in the lockdown period. The major source of NO_2 is vehicular emissions and it shows high concentration in urban regions. The NO_x emissions in Delhi due to passenger cars were reported to be ~50%[41] and the on-road $PM_{2.5}$ concentrations were more than 50% of ambient concentrations.[42] The average NO_2 concentrations in Delhi during the pre- and first lockdown periods in 2020 and 2021 are illustrated in Fig. 3. With 90% of vehicles off the road during the lockdown period, NO_2 concentration was below 40 μg m^{-3} and there were days in 2020 when the NO_2 concentration was even below 20 μg m^{-3}. Thus on an average, NO_2 emissions decreased during lockdown.

Atmospheric photooxidation of species emitted into the atmosphere (predominantly volatile organic compounds, VOCs) from natural and anthropogenic sources is initiated mainly by OH radicals, which are atmospheric bleaching agents. An overview of atmospheric oxidation chemistry is shown in Fig. 4. The products resulting from these oxidation reactions are affected by the concentration of primary pollutants and other species emitted into the atmosphere. Thus, the NO_2 concentration in the atmosphere plays a significant role in atmospheric oxidation chemistry. Atmospheric oxidation initiated by oxidants results in peroxy radicals as the key intermediate and NO_x controls the fate of these peroxy radicals. In high-NO_x conditions, O_3 is formed through photolysis of NO_2, as shown in (R1) and (R2), whereas in low-NO_x conditions self-reaction or isomerization of peroxy radicals takes place. The rate of formation of ozone through NO_2 photolysis also depends on the concentration of VOCs and the dependence is complex and non-linear.[43] That is, in cases of high VOC concentration and low NO_x levels, the chemistry is NO_x-limited and in this situation more NO_x leads to more O_3 production. In contrast, at higher NO_x concentrations, the oxidation of VOCs slows down and O_3 production is suppressed. Thus in this case, more NO_x does not lead to more O_3. This is well reflected in the air pollution data during the lockdown period in all the regions studied, where NO_x emissions decreased but O_3 emissions were at their peak. As shown in Fig. 4, $PM_{2.5}$ levels depend on the levels of its precursors, such as VOCs, SO_2, and NO_2 and their oxidation chemistry in the atmosphere. In the studied regions, the correlations of NO_2 with $PM_{2.5}$ and PM_{10} are positive (Fig. 2), showing the effects of precursor changes on $PM_{2.5}$ and PM_{10}. In the case of Delhi and Pune, SO_2 levels are positively correlated

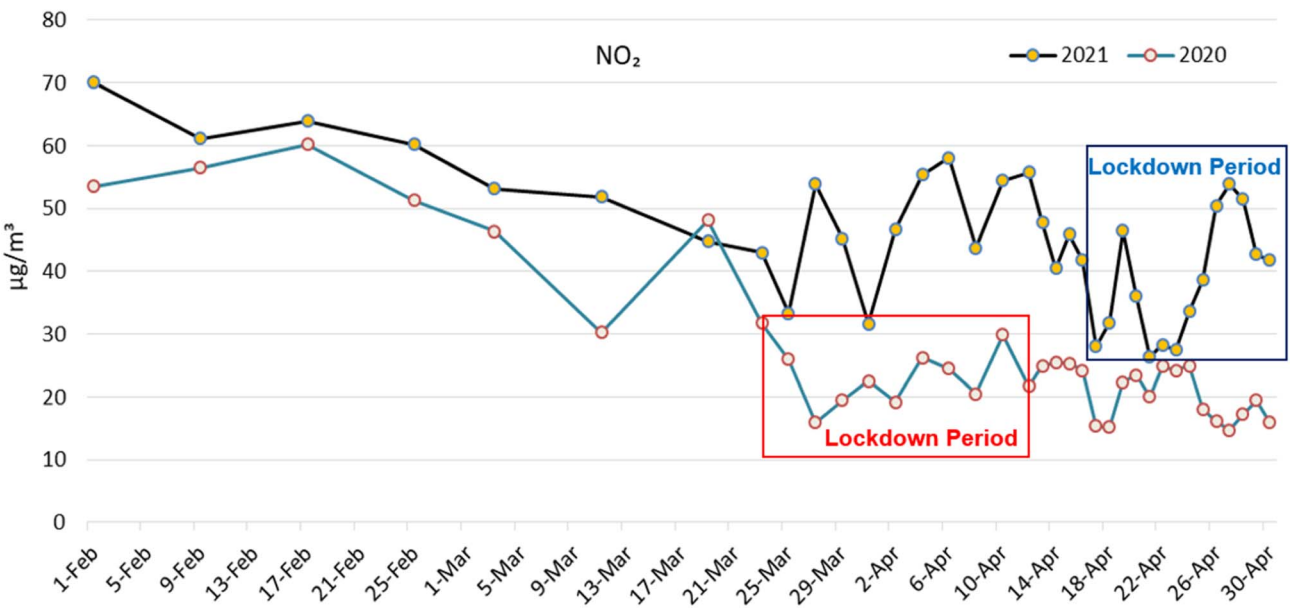

Fig. 3 Average NO_2 concentrations during the pre-lockdown and lockdown periods in Delhi in 2020 and 2021.

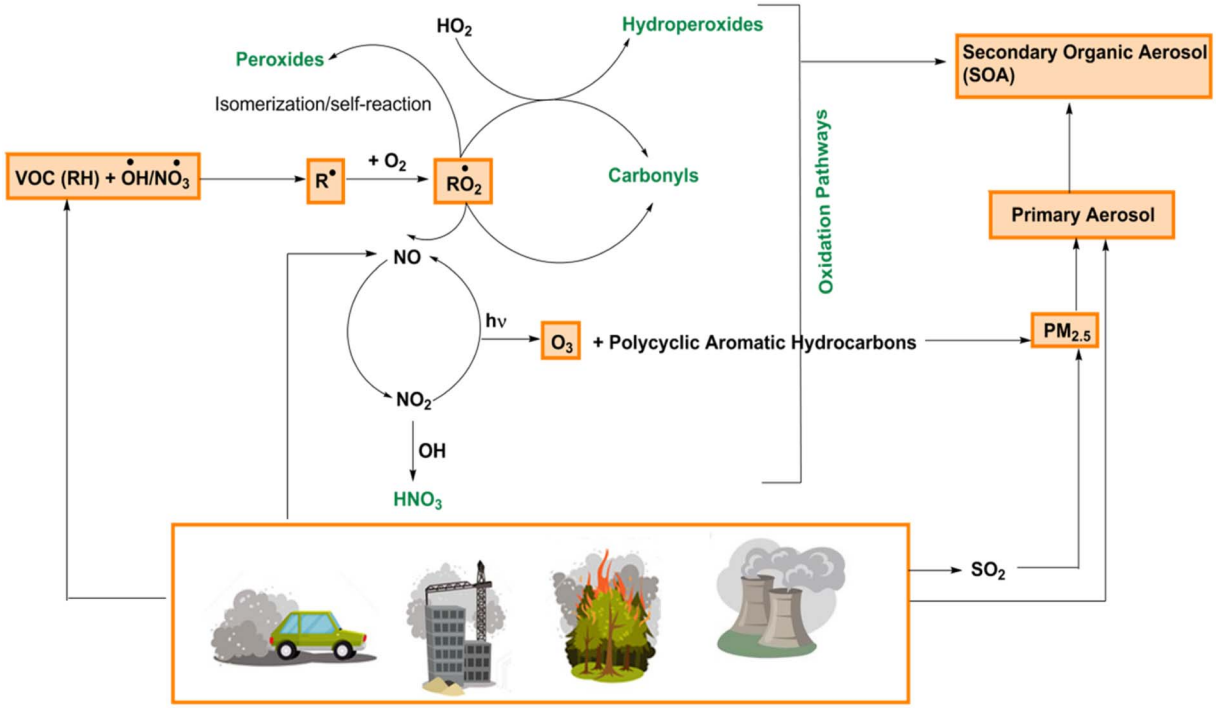

Fig. 4 Outline of atmospheric oxidation processes leading to secondary pollutants.

with $PM_{2.5}$ and PM_{10}, whereas in Assam and Trivandrum, the correlations are weak and negative, respectively.

The above discussions reveal that the chemical composition of the atmosphere is complex and the complexity increases with different mechanistic pathways leading to multiple products. Overall, from Fig. 1–4, it is inferred that on assessing the air quality during the COVID-19 lockdown and deriving the relationship between dispersion of pollutants and the spread of the virus, O_3 and particulate matter are two major pollutants that can improve the process-level understanding of the impact of air pollutants on the spread of infectious viruses. Furthermore, the effect of O_3 and $PM_{2.5}$ on the deposition of SARS-CoV-2 aerosols in the respiratory system may aid in understanding the linkages between air pollutants and infectious aerosols.

3.3 Climate factors

Airborne viruses that are transmitted in air undergo dilution, but in polluted atmosphere the viruses accumulate, depending upon climate factors, such as temperature, RH, wind speed and evaporation. In the following section we consider Delhi as a prototype to discuss the impact of climate parameters on the dispersion of SARS-CoV2 aerosols. Since Delhi is an ideal representative for high pollutant concentrations and large numbers of COVID-19 infections and fatalities in the second wave, the effects of climate factors in Delhi on the infections are studied in detail. The influence of meteorology on the dispersion of SARS-CoV2 aerosols is different for the different cities studied. Owing to the lack of data in other regions, the influence of climate factors on the dispersion of SARS-CoV2 aerosols in Delhi is considered in the present study. The average of the average daily temperature, relative humidity, wind intensity and evaporation for the period of analysis (16 March to 31 May 2021) are 36.9 ± 3.62 °C, $70.4 \pm 10.59\%$, 5.2 ± 2.27 km h^{-1} and 7.1 ± 1.95 mm, respectively. The aerosols produced by sneezing and coughing are initially expelled from the respiratory tract in air at a temperature of 31 °C. At the average temperature of ~37 °C in Delhi during the analysed period, there is a slight probability for the expelled droplets to remain airborne. The virus-laden aerosols settle in the atmosphere with intensities ranging from 2.8×10^{-5} m s^{-1} to 1.4×10^{-3} m s^{-1} for aerosol sizes of 1 and 10 μm, respectively.[44] The average wind speed during the analysed period was 1.44 m s^{-1} which can be compared with the intensity of large aerosols (10 μm) of wind speed 1.4×10^{-3} m s^{-1}, revealing that virus-bearing larger aerosols do not mix with air and the residence times for these aerosols are short and they transmit the virus over relatively short distances. The average RH of $70.4 \pm 10.59\%$ observed during the period of analysis has the capability to evaporate the expelled droplets,[45] which would reduce the size of the droplets and that of the resulting aerosols. As discussed earlier, these smaller aerosols possess a long lifetime in air. A recent estimate[46] showed that an RH of 50% can lead to drying of droplets with an initial size of <40 μm through water loss before they fall to the ground. This water loss could affect the stability of the pathogens which are present in the droplet.[47] The dry droplets thus suspended in air produce aerosols loaded with virions which remain airborne. Furthermore, the high ambient RH of >60% observed in Delhi during the analysed period created a humid microenvironment enhanced by the cloud and this had greater potential to stimulate the infectivity of respiratory viruses before dispersion in air.[20]

Table 1 Pearson coefficients for correlation between COVID-19 cases and climate factors in Delhi

	Temperature (°C)		Wind intensity (km h^{-1})		RH (%)		Evaporation rate (mm d^{-1})	
COVID-19 cases	Pearson	*p*-Value	Pearson	*p*-Value	Pearson	*p*-Value	Pearson	*p*-Value
Daily fresh cases	0.43	<0.01	0.03	0.73	−0.39	<0.01	0.39	<0.01
Deaths	0.37	<0.01	0.004	0.97	−0.34	0.001	0.78	0
Total number of cases	0.17	0.12	0.05	0.64	−0.18	0.10	0.88	0

The Pearson coefficients for correlation between daily fresh cases, daily deaths and total number of cases in Delhi for the analyzed period are listed in Table 1. The temperature, wind intensity and evaporation rate are positively correlated with COVID-19 infections and fatalities, whereas RH is negatively correlated. The statistical correlation showed that wind intensity and evaporation rate have significant *p*-values, implying that these factors might be significant for SARS-CoV-2 aerosol transmission.

To gain more understanding of the possible association between the transmission of COVID-19 and meteorological factors, the variation in the 7 day average of COVID-19-positive cases in relation to the RH observed on the day was studied (see Fig. 6). Since RH and ozone are strongly correlated, the evolution of 7 day average COVID-19 cases and average O_3 was also studied.

As is evident from Fig. 6, during the peak COVID-19 period, the average O_3 concentration levels were at their peak and the corresponding RH levels were at a minimum. This is again suggestive of the fact that relatively low humidity levels lead to the maximum production of secondary ozone through photochemical processes. This is further confirmed by the Pearson correlation coefficient, which shows a strong negative correlation of -0.44 and $p = 10^{-4}$ between the two variables. Daily averaged O_3 concentration levels exhibited extreme correlation with 7 day-averaged COVID-19 cases with a Pearson coefficient of 0.51, $p = 10^{-6}$. The RH is strongly negatively correlated with 7 day-averaged COVID-19 cases (Pearson correlation $= -0.42$, $p = 10^{-4}$). At high RH level, there is a high possibility that ozone deposition on water droplets[30] or virion droplets will take place. Thus, the daily variations in RH and O_3 are well correlated with the changes in the number of COVID-19 cases, and RH may modulate the transmission of COVID-19 through ozone production.

3.4 Aerosol deposition in the lung

As discussed above, the air pollution resulting from high O_3 concentration significantly increases the risk of respiratory diseases. SARS-CoV-2-virus-laden aerosols in the atmosphere undergo reactive encounters with atmospheric oxidants and form SOAs before deposition in the lung, which is a multiscale and multiphysical/multichemical process. Hence, it remains a challenge to identify all possible physical/chemical pathways that contribute to the deposition of SARS-CoV-2-virus-laden aerosols in the lung. Owing to the positive correlation of O_3 with SARS-CoV-2 infections, we attempt here to provide a mechanism for the interaction of atmospheric O_3 and SOA with the respiratory system, which would trigger free radical formation. The major components in a respiratory droplet are salt, protein and surfactant and the physico-chemical characteristics of these droplets in ambient air affect the sustainability of any pathogens contained within the droplet.[48] Here we focus on the interaction of atmospheric O_3 with lung surfactant. The lung epithelium biosurface/surfactant with fluid linings containing antioxidants is a natural shield against atmospheric ozone. Antioxidants, such as ascorbic acid (AH_2), uric acid (UA), glutathione (GSH) and α-tocopherol are the major interfacial fluids on the biosurface which prevent atmospheric O_3 reaching the underlying tissues. Atmospheric O_3 may cause oxidative stress to the lungs if it is not scavenged by these antioxidants on the biosurface before reaching the lung cells. That is, the co-pollutants/SOA can enhance and transmit the antioxidants and gaseous O_3 to produce new species resulting in oxidative damage to the tissues. AH_2 and UA are the most important antioxidants present in high concentrations in both the upper and lower regions of the respiratory tract. The reactivities of gaseous O_3 with AH_2 and UA are of the same order, but in aqueous solution the reaction between AH_2 and O_3 is faster with a rate coefficient of 10^7 M^{-1} s^{-1}. AH_2 forms the first ring of defense against ozone in intercellular fluid.[49] The ozonolysis of AH_2 initially forms a primary ozonide which rearranges into a secondary ozonide and forms different secondary oxidation products. This secondary oxidation, if forcefully transduced across the epithelial lining fluid, rapidly diffuses through a fluid layer of ~0.1 μm thickness.[50]

The mechanism for the reaction between AH_2 and O_3 is studied using density functional theory at DFT-UM06-2X/6-311+G(d,p) level of theory and the potential energy surface is shown in Fig. 7. The reaction proceeds by the addition of O_3 to the C=C bond of AH_2, resulting in the formation of a primary ozonide (**INT1**) in an extremely exothermic reaction of -75.3 kcal mol^{-1} enthalpy. The polar solvation and the reaction in lipid medium show that the primary ozonide is formed with 10 kcal mol^{-1} less exothermicity than that in the gas phase. The reaction initially forms a pre-reactive complex which is 12.3 kcal mol^{-1} more stable than the separated reactants in the gas phase. In solvent medium, the pre-reactive complex is weakly bound and less stable than that in the gas phase. The enthalpy barriers for the formation of **INT1** through transition state TS1 are 4.1, 3.7 and 3.9 kcal mol^{-1} in gas, aqueous and lipid media, respectively. This reveals that the reaction is equally feasible in gas, aqueous and lipid media. The relatively low energy barrier

and the thermodynamic driving force enable the primary ozonide to diffuse through the lung-lining fluid and trigger inflammatory responses.[51] The **INT1** so formed loses resonance stabilization and hence it is a weaker acid than the parent AH_2. However, the inhalation of acidic airborne particles locally acidifies the primary ozonide and thus AH_2 loses its efficiency toward O_3 scavenging.[52] **INT1** undergoes decomposition through C–C and O–O bond dissociation to a Criegee intermediate (**INT2**) in an extremely exothermic reaction with −94.1, −90.9 and −85.5 kcal mol^{-1} enthalpy, respectively, in gas, aqueous and lipid media. The enthalpy barriers required for this process are 37.7, 17.7 and 21.1 kcal mol^{-1}, respectively, through TS2 in the three media. The Criegee intermediate further rearranges into a secondary ozonide (**P1**) with reaction enthalpies of −50.8, −47.3 and −42.2 kcal mol^{-1} in the three phases. The secondary ozonide is a stronger acid than the primary ozonide with the formation of two C–O bonds in a bridge. **P1** can undergo further unimolecular dissociation resulting in new fragments. **P1** is formed through a ring-closure transition state TS3, which requires 74.1, 78.6 and 74.6 kcal mol^{-1} enthalpy barriers in gas, aqueous and lipid media, respectively, with respect to **INT2**. The calculated enthalpy barrier and the reaction enthalpy show that primary ozonide **INT1** is the most favourable product formed by the ozonolysis of AH_2 in gas as well as in solvent media. Although the Criegee intermediate **INT2** and secondary ozonide **P1** are largely enthalpy driven, the pronounced kinetic barrier in the formation of the product makes this secondary pathway less feasible in AH_2 ozonolysis.

Atmospheric O_3 interacts with the lung-lining fluids through interfacial layers which are mostly air–water or air–acidic water interfaces, that can be mimicked as a droplet–air interface. From the PES shown above, it is inferred that the acidity of ascorbic acid and its secondary products play an important role in determining the degree of O_3 scavenging. An earlier experimental study showed that the reaction between ascorbic acid and O_3 is competitive with O_3 desorption at the air–water interface.[53] Taking the theoretical and experimental results together, it is important to understand how acidity changes through the interfacial layer. First, we look at the thermodynamics of proton transfer from ascorbic acid to H_2O or OH^- in the gas phase, as given in the reactions below:

$$\begin{aligned} AH_2(g) + H_2O(g) &= AH^-(g) + H_3O^+(g), \\ \Delta H_{298}\ [\text{kcal mol}^{-1}] &= 153.5, \\ \Delta G_{298}\ [\text{kcal mol}^{-1}] &= 153.2 \end{aligned} \quad \text{(R5)}$$

$$\begin{aligned} AH_2(g) + OH^-(g) &= AH^-(g) + H_2O(g), \\ \Delta H_{298}\ [\text{kcal mol}^{-1}] &= -74.1, \\ \Delta G_{298}\ [\text{kcal mol}^{-1}] &= -79.9 \end{aligned} \quad \text{(R6)}$$

When the lung-lining fluid is neutral (pH ≈ 7), ascorbate anions (AH^-) formed through proton transfer reactions can convert O_3 to innocuous dehydrated ascorbate. As shown above, (R6) is thermodynamically more favourable than (R5), showing that the reaction can occur feasibly at the air–water interface. (R5), where infinitely separate ions are produced from neutral species, is largely endothermic and endoergic. Earlier studies showed that the endoergicity in the proton transfer reaction from carboxylic acid to H_2O can be reduced to ∼100 kcal mol^{-1}, when the products are ion-pairs in the early stages of proton transfer.[54,55] It has also been shown that the participation of an additional six H_2O molecules leads to contact ion-pairs that can make the reaction exoergic.[56] Hence, considering these arguments we performed quantum chemical calculations of the proton transfer reaction from ascorbic acid to H_2O or OH^- on water clusters. Here 10 water molecules $(H_2O)_{10}$ were chosen to form a cluster with OH^- ions, $(H_2O)_{10}\cdot OH^-$. The UM06-2X/6-311+G(d,p) level of theory were used for this modelling. The calculated enthalpies for proton transfer between AH_2 and the $(H_2O)_{10}\cdot OH^-$ cluster and that with O_3 adsorbed on the surface and the formation of primary and secondary ozonides on the surface are presented in Fig. 8.

The adsorption of AH_2 on the $(H_2O)_{10}\cdot OH^-$ cluster occurs through an H-bonding interaction between one hydroxyl group of AH_2 and one water molecule and the complex is strongly bound by −40.1 kcal mol^{-1} enthalpy. The proton transfer between AH_2 and the $(H_2O)_{10}\cdot OH^-$ cluster takes place through proton transfer to the OH^- ion of the cluster involving H-bonding interactions with three water molecules. The resulting $AH^-\cdot(H_2O)_{11}$ complex is stable with −49.3 kcal mol^{-1} enthalpy. Proton transfer in the absence of OH^- ions did not lead to AH^- + H_3O^+ dissociation products. Proton transfer leading to an $AH^-\cdot(H_2O)_{11}$ complex with O_3 adsorbed on the

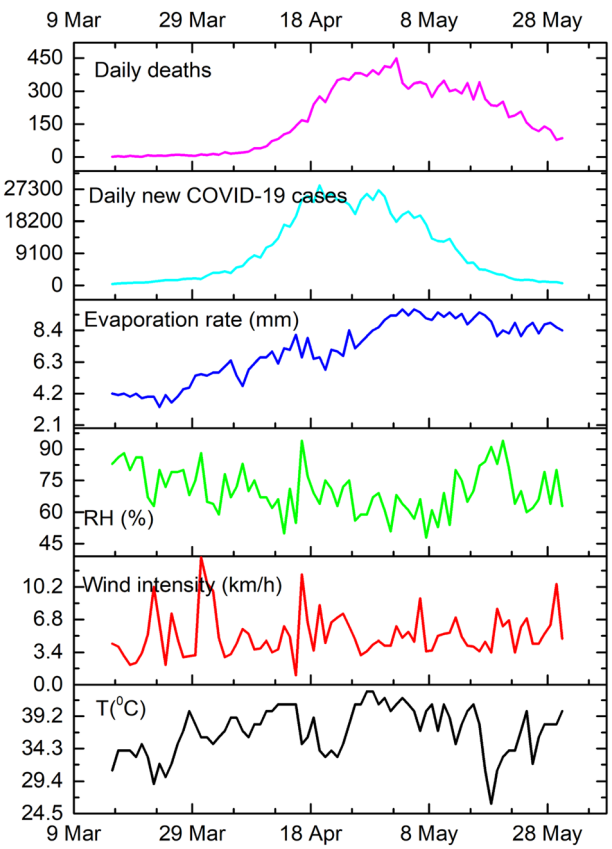

Fig. 5 Patterns of daily averaged climate variables with the daily number of COVID-19 cases and fatalities in Delhi.

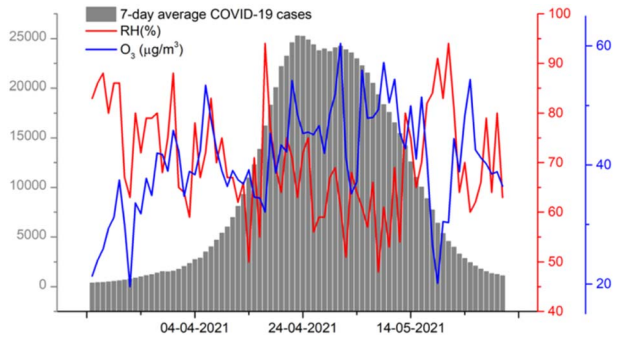

Fig. 6 Variation of 7 day-averaged COVID-19 cases relative to the RH and average O_3 observed on the day.

surface is exothermic with −57.2 kcal mol^{-1} enthalpy. This is 7.9 kcal mol^{-1} more exothermic than a proton transfer reaction on the surface without the presence of O_3. Furthermore, two water molecules and an OH^- ion are involved in this proton transfer reaction, which may result in a negligible kinetic barrier for the formation of a stable $[AH^- \cdot (H_2O)_{11} \cdot O_3]$ complex. The reaction of AH^- with O_3 on the water surface results in proton exchange, leading to dehydroxy ascorbic acid (DHA) along with singlet oxygen and a hydroxide ion. This reaction is, however, less significant in the AH_2 ozonolysis reaction due to high-lying $^1O_2$.

When the lung-lining fluid is acidic due to the inhalation of acidic aerosols, AH_2 reacts with O_3, leading to ozonide and other toxic products. The formation of primary ozonide **INT1** on the surface $[(\mathbf{INT1}) \cdot (H_2O)_{10} \cdot (OH^-)]$ is extremely exothermic by −112.5 kcal mol^{-1}, which is ∼37 kcal mol more exothermic than the formation of **INT1** in the gas phase. This reveals the strong plausibility for the formation of primary ozonide at the air–water interface. The complex $[(\mathbf{INT1}) \cdot (H_2O)_{10} \cdot (OH^-)]$ involves a hydrogen-bonding interaction between two hydroxyl groups of **INT1** with two H_2O molecules of the surface and the OH^- ion resides at the surface of the water cluster. The primary ozonide adsorbed on the water droplet at the air–water interface thus possesses greater potential to serve as a silent secondary aerosol that penetrates through the epithelium and prompts inflammatory responses. The secondary ozonide **P1** is formed on the surface $[(\mathbf{P1}) \cdot (H_2O)_{10} \cdot (OH^-)]$ with −85.7 kcal mol^{-1} exothermicity, where a single H-bonding interaction is observed between **P1** and the surface. The **P1** formed on the surface is ∼35 kcal mol^{-1} more exothermic than that in the gas phase. This reaction occurs mainly from Criegee intermediate **INT2** formed in the gas phase and undergoes hydration at the interface through heterogeneous processes. This mechanism is interface-specific and depends on the bulk pH values ranging from 1 to 11.[57] Determining the mechanism with different pH values will result in the identification of the other toxic products formed at the air–water interface and this is out of the scope of the present study.

Together with these preliminary findings of the dispersion of virus-laden aerosols in air and their interaction with lung-lining fluids and along with earlier observations,[53,55] the relevance of

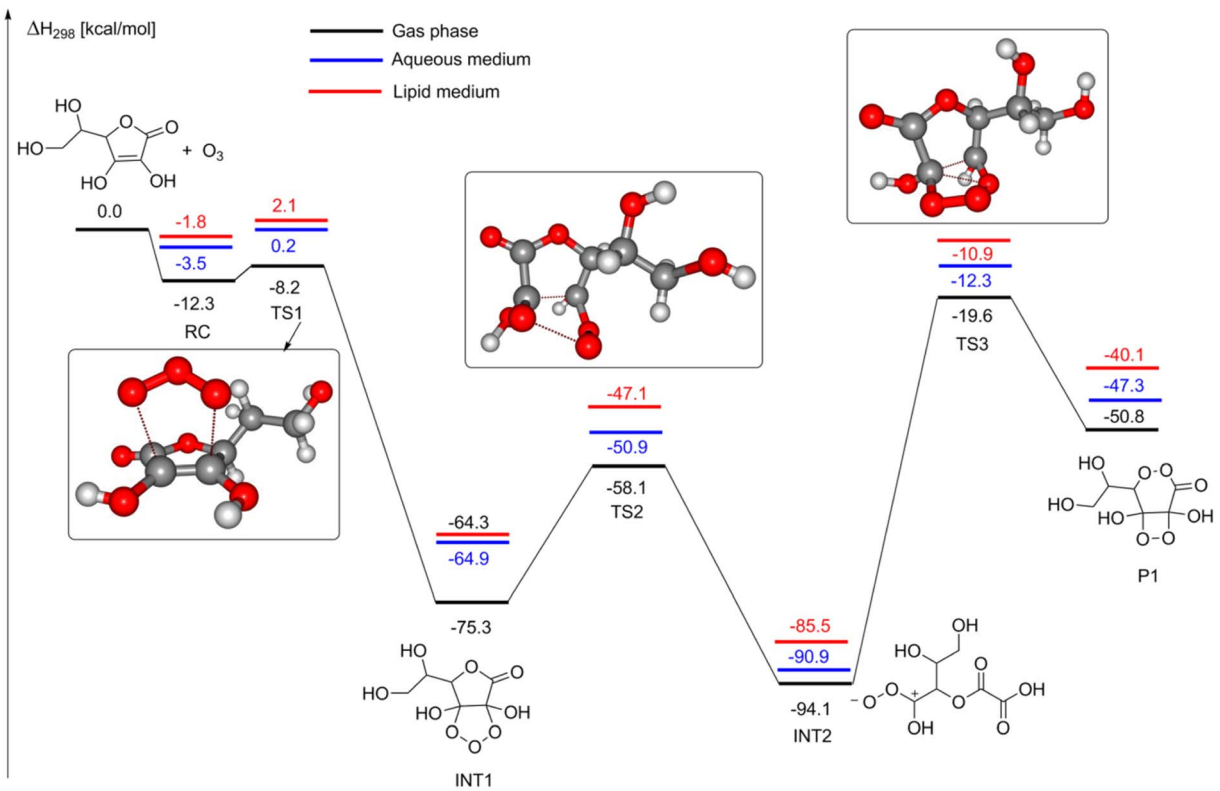

Fig. 7 PES for ascorbic acid ozonolysis in gas, aqueous and lipid media.

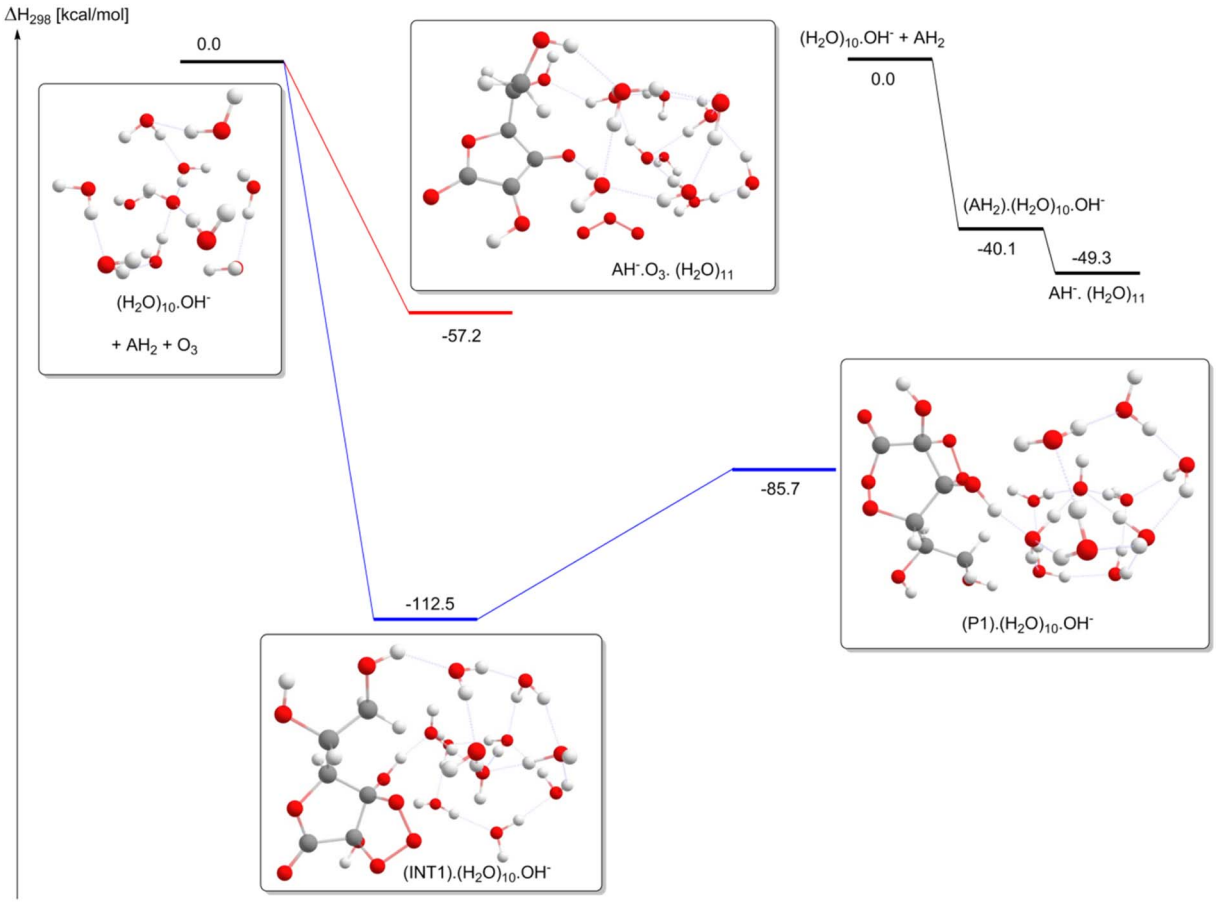

Fig. 8 Enthalpies (ΔH_{298}, kcal mol^{-1}) calculated for the reactions between ascorbic acid and O_3 on the [$(H_2O)_{10}\cdot OH^-$] surface.

the impact of O_3 on the deposition of SARS-CoV-2 aerosols is emphasized. Lung tissues simultaneously exposed to O_3 and acidic aerosols enhanced oxidative stress upon breathing[58,59] due to the formation of energetically accessible primary ozonide **INT1**, as shown in Fig. 5 and 6. The C-centered radical intermediate **INT2** formed with large exothermicity and the secondary ozonide **P1** caused acute responses *in vivo*.[60] The results show the fundamental connection between the gaseous co-pollutants and aerosol acidity in the deposition of virus-loadings in the lungs. Epidemiological and toxicological studies in this direction are required to understand the connectivity between air pollution and its impacts on SARS-CoV-2 transmission and deposition.

4. Conclusions

A multidisciplinary approach involving different disciplines of science and engineering is required to eradicate SARS-CoV-2. In this direction, the present study provides vital information on possible linkages between air pollution and climate factors in the dispersion and deposition of SARS-CoV-2 aerosols by using statistical analysis and electronic structure calculations. As airborne transmission through aerosols is debated to be one possible pathway for the spread of coronavirus, the present study provides a comprehensive analysis of the impact of air pollutants such as O_3, NO_2, $PM_{2.5}$, PM_{10} and SO_2, with a particular emphasis on the impact of ground-level ozone and NO_2 in the dispersion and deposition of SARS-CoV-2 aerosols. Four different sites with different climate zones in India were chosen for the study. In most cases, COVID-19 infections and fatalities correlated with $PM_{2.5}$, NO_2 and PM_{10} concentrations. In the case of Delhi, during the peak COVID-19 period, the average ground-level ozone concentration was elevated by 20.4% and the average NO_2 concentration decreased by 25.9%. Furthermore, the impact of meteorological factors on the spread of infectious aerosols was also analyzed. The relative humidity (RH) showed a strong negative correlation with daily number of infections as well as 7 day-averaged COVID-19-positive cases. During the peak COVID-19 period, the RH levels were low while the average ozone levels were higher. This suggests that RH may modulate the transmission of SARS-CoV-2 aerosols by modulating ozone production.

Long-term exposure to air pollutants is considered a possible carrier of infections and has negative impacts on the human immune and respiratory system. Owing to the positive correlation between average O_3 concentration and COVID-19 infections and mortality, the impact of O_3 on the deposition of SARS-

CoV-2 aerosols was studied. For this, the interaction of the lung-lining fluid antioxidant ascorbic acid with O_3 was studied using electronic structure calculations in gas, aqueous and lipid phases. The results show that primary ozonide is formed as the main intermediate in the first step, in a reaction that is both kinetically and thermodynamically favourable. The primary ozonide has sufficient internal energy to dissociate to toxic secondary products. Furthermore, the acidity of ascorbic acid and its secondary products plays an important role in the scavenging of O_3 in the lung epithelium. In order to study the interaction of acidic aerosols with O_3 at the air–water interface, the thermochemistry of the reactions on the surface of a water cluster along with an OH^- ion was calculated. At the air–water interface, persistent primary ozonide was formed much more energetically favourably than in the gas, aqueous or lipid phases. This clearly shows that within the epithelium lung fluid, if there are pre-existing pathologies that lead to respiratory diseases, the inhalation of acidic airborne particles further acidifies the lung-lining fluids. Thus, because of primary ozonide formation, ascorbic acid loses its efficiency to scavenge O_3. Further concern is due to secondary particulate matter, which is more acidic and inhaled through the airways, making the epithelium more acidic, thereby reducing the scavenging activity of antioxidants. Hence, the interaction of secondary particulate matter and other co-pollutants with lung-lining fluids positively influences the deposition of infectious aerosols in the lungs.

Chemically speaking, the dispersion and deposition of aerosols are multiphase and heterogeneous processes that involve several chemical species and their interaction in different environments and surfaces. Physically speaking, the deposition of inhaled virus-laden aerosols in different parts of the respiratory system is influenced by their size, density, shape, charge, hydrophobicity and hygroscopicity.[61] Thus, the dispersion and deposition of SARS-CoV-2-laden aerosols are complex phenomena, that require further epidemiological and toxicological studies to elucidate the association between air pollutants and SARS-CoV-2. The current study provides a base to understand the possible association of atmospheric conditions and pollutants, particularly ozone concentrations and RH in the transmission of SARS-CoV-2 aerosols and the impact of their subsequent deposition in the respiratory tract.

Author contributions

Sandhiya Lakshmanan: conceptualization, methodology, writing original-draft preparation, reviewing and editing. Ranjana Aggarwal: co-supervision, data analysis, reviewing. Kittusamy Senthilkumar: co-supervision, data analysis, reviewing and editing. Anupama: data analysis, graphical representation.

Conflicts of interest

The authors declare that they have no known competing financial interests or personal relationships that could have appeared to influence the work reported in this paper.

Acknowledgements

The authors acknowledge Central Pollution Control Board (CPCB), India for providing air pollution data.

References

1 World Health Organization (WHO), *Coronavirus disease 2019 (COVID-19) situation report-51*, 2020, **https://www.who.int/emergencies/diseases/novel-coronavirus-2019/situationreports**.
2 J. Cai, W. Sun, J. Huang, M. Gamber, J. Wu and G. He, *Emerging Infect. Dis.*, 2020, **26**, 1343–1345.
3 M. Jayaweera, H. Perera, B. Gunawardana and J. Manatunge, *Environ. Res.*, 2020, **188**, 109819.
4 N. van Doremalen, T. Bushmaker, D. H. Morris, M. G. Holbrook, A. Gamble, B. N. Williamson, A. Tamin, J. L. Harcourt, N. J. Thornburg, S. I. Gerber, J. O. Lloyd-Smith, E. D. Wit and V. J. Munster, *N. Engl. J. Med.*, 2020, **382**, 1564–1567.
5 A. W. H. Chin, J. T. S. Chu, M. R. A. Perera, K. P. Y. Hui, H. L. Yen, M. C. W. Chan, M. Peiris and L. L. M. Poon, *Lancet*, 2020, **1**, E10.
6 R. Zhang, Y. Li, A. L. Zhang, Y. Wang and M. J. Molina, *Proc. Natl. Acad. Sci. U. S. A.*, 2020, **117**, 14857–14863.
7 R. Mittal, R. Ni and J. H. Seo, *J. Fluid Mech.*, 2020, **894**, F2-1–F2-14.
8 M. Riediker and D.-H. Tsai, *JAMA Netw. Open*, 2020, **3**, e2013807.
9 S. Asadi, A. S. Wexler, C. D. Cappa, S. Barreda, N. M. Bouvier and W. D. Ristenpart, *PLoS One*, 2020, **15**, e0227699.
10 M. Nicas, W. W. Nazaroff and A. Hubbard, *J. Occup. Environ. Hyg.*, 2005, **2**, 143–154.
11 L. Morawska, G. R. Johnson, Z. D. Ristovski, M. Hargreaves, K. Mengersen, S. Corbett, C. Y. H. Chao, Y. Li and D. Katoshevski, *J. Aerosol Sci.*, 2009, **40**, 256–269.
12 S. Yang, G. W. M. Lee, C.-M. Chen, C.-C. Wu and K.-P. Yu, *J. Aerosol Med.*, 2007, **20**, 484–494.
13 GesellschaftFürAerosolforschung, e.V., *Position Paper of the GesellschaftfürAerosolforschung on Understanding the Role of Aerosol Particles in SARS-CoV-2 Infection*, Assoc. Aerosol Res., 2020.
14 W. Chen, N. Zhang, J. Wei, H.-L. Yen and Y. Li, *Build. Environ.*, 2020, **176**, 106859.
15 M. Evans, Avoiding COVID-19: Aerosol Guidelines, *medRxiv*, 2020, preprint, ver. 1, arXiv:2005.10988, DOI: **10.48550/arXiv.2005.10988**.
16 Y. Y. Zuo, W. E. Uspal and T. Wei, *ACS Nano*, 2020, **14**, 16502–16524.
17 G. Buonanno, L. Morawska and L. Stabile, *Environ. Int.*, 2020, **145**, 106112.
18 R. Tellier, *J. R. Soc., Interface*, 2009, **6**(suppl. 6), S783–S790.
19 L. Bourouiba, E. Dehandschoewercker and J. W. M. Bush, *J. Fluid Mech.*, 2014, **745**, 537–563.
20 M. Moriyama, W. J. Hugentobler and A. Iwasaki, *Annu. Rev. Virol.*, 2020, **7**, 83–101.

21 D. Liang, L. Shi, J. Zhao, P. Liu, J. Schwartz, S. Gao, J. A. Sarnat, Y. Liu, S. T. Ebelt, N. C. Scovronick and H. Chang, *Innovation*, 2020, **1**, 100047.
22 E. Conticini, B. Frediani and D. Caro, *Environ. Pollut.*, 2020, **261**, 114465.
23 X. Wu, R. C. Nethery, M. B. Sabath, D. Braun and F. Dominici, *Sci. Adv.*, 2020, **6**, eabd4049.
24 Y. Yin and R. G. Wunderink, *Respirology*, 2018, **23**, 130–137.
25 J. V. Fahy and B. F. Dickey, *N. Engl. J. Med.*, 2010, **363**, 2233–2247.
26 C. A. Ruge, J. Kirch and C. M. Lehr, *Lancet Respir. Med.*, 2013, **1**, 402–413.
27 L. Sandhiya, P. Kolandaivel and K. Senthilkumar, *J. Phys. Chem. B*, 2014, **118**, 3479–3490.
28 T. Franze, M. G. Weller, R. Niessner and U. Poschl, *Environ. Sci. Technol.*, 2005, **39**, 1673–1678.
29 P. Asrani, M. S. Eapen, M. I. Hassan and S. S. Sohal, *Lancet Respir. Med.*, 2021, **9**, e93–e94.
30 N. Korhale, V. Anand and G. Beig, *Air Qual., Atmos. Health*, 2021, **14**, 533–542.
31 P. R. Nair, R. S. Ajayakumar, L. M. David, I. A. Girach and K. Mottungan, *Environ. Sci. Pollut. Res.*, 2018, **25**, 14827–14843.
32 U. C. Dumka, A. S. Gautam, S. Tiwari, D. S. Mahar, S. D. Attri, R. K. Chakrabarty, P. Permita, P. K. Hopke and R. Hooda, *Atmos. Pollut. Res.*, 2021, **11**, 610–618.
33 Y. Zhao and D. G. Truhlar, *Theor. Chem. Acc.*, 2008, **120**, 215–241.
34 M. J. Frisch, *et al.*, *Gaussian 09, Revision D.01*, Gaussian, Inc., Wallingford CT, 2009.
35 S. Mahato, S. Pal and K. G. Ghosh, *Sci. Total Environ.*, 2020, **730**, 139086.
36 A. K. Gorai, P. B. Tchounwou and G. Mitra, *Aerosol Air Qual. Res.*, 2017, **17**(4), 951.
37 S. He and G. R. Carmichael, *J. Geophys. Res.*, 1999, **104**, 26307–26324.
38 C. George, M. Ammann, B. D'Anna, D. J. Donaldson and S. A. Nizkorodov, *Chem. Rev.*, 2015, **115**, 4218–4258.
39 M. A. Zoran, R. S. Savastru, D. M. Savastru and M. N. Tautan, *Sci. Total Environ.*, 2020, **740**, 140005.
40 S. Shi, M. Qin, B. Shen, Y. Cai, T. Liu, F. Yang, W. Gong, X. Liu, J. Liang, Q. Zhao, H. Huang, B. Yang and C. Huang, *JAMA Cardiol.*, 2020, **5**(7), 802–810.
41 P. Goyal, D. Mishra and A. Kumar, *SpringerPlus*, 2013, **216**, 1–11.
42 J. S. Apte, T. W. Kirchstetter, A. H. Reich, S. J. Deshpande, G. Kaushik, A. Chel, J. D. Marshall and W. W. Nazaroff, *Atmos. Environ.*, 2011, **45**, 4470e4480.
43 J. H. Kroll, C. L. Heald, C. D. Cappa, D. K. Farmer, J. L. Fry, J. G. Murphy and A. L. Steiner, *Nat. Chem.*, 2020, **12**, 777–779.
44 R. Zhang, G. Wang, S. Guo, M. L. Zamora, Q. Ying, Y. Lin, W. Wang, M. Hu and Y. Wang, *Chem. Rev.*, 2015, **115**, 3803–3855.
45 R. R. Netz, *J. Phys. Chem. B*, 2020, **124**, 7093–7101.
46 R. R. Netz and W. A. Eaton, *Proc. Natl. Acad. Sci. U. S. A.*, 2020, **117**, 25209–25211.
47 G. E. Carpagnano, M. P. Foschino-Barbaro, C. Crocetta, D. Lacedonia, V. Saliani, L. D. Zoppo and P. J. Barnes, *Chest*, 2017, **151**, 855–860.
48 P. E. Vejerano and L. C. Marr, *J. R. Soc., Interface*, 2018, **15**, 20170939.
49 Y. K. Sharma and K. R. Davis, *Free Radical Biol. Med.*, 1997, **23**, 480–488.
50 W. A. Pryor, *Free Radical Biol. Med.*, 1992, **12**, 83–88.
51 C. A. Ballinger, R. Cueto, G. Squadrito, J. F. Coffin, L. W. Velsor, W. A. Pryor and E. M. Postlethwait, *Free Radical Biol. Med.*, 2005, **38**, 515–526.
52 M. Lippmann, *N. Engl. J. Med.*, 2007, **357**, 2395–2397.
53 S. Enami, M. R. Hoffmann and A. J. Colussi, *Proc. Natl. Acad. Sci. U. S. A.*, 2012, **109**, 7365–7369.
54 K. R. Leopold, *Annu. Rev. Phys. Chem.*, 2011, **62**, 327–349.
55 H. Mishra, S. Enami, R. J. Nielsen, L. A. Stewart, M. R. Hoffmann, W. A. Goddard III and A. J. Colussi, *Proc. Natl. Acad. Sci. U. S. A.*, 2012, **109**, 18679–18683.
56 M. Meot-Ner, *Chem. Rev.*, 2005, **105**, 213–284.
57 J. Qiu, S. Ishizuka, K. Tonokura, K. Sato, S. Inomata and S. Enami, *J. Phys. Chem. A*, 2019, **123**, 7148–7155.
58 J. A. Last, *Environ. Health Perspect.*, 1991, **96**, 151–157.
59 L. C. Chen, P. D. Miller, H. F. Lam, J. Guty and M. O. Amdur, *J. Toxicol. Environ. Health*, 1991, **34**, 337–352.
60 Y. Tang, Y. Dong, S. Wittlin, S. A. Charman, J. Chollet, F. C. K. Chiu, W. N. Charman, H. Matile, H. Urwyler, A. Dorn, S. Bajpai, X. Wang, M. Padmanilayam, J. M. Karle, R. Brun and J. L. Vennerstrom, *Bioorg. Med. Chem. Lett.*, 2007, **17**(5), 1260–1265.
61 J. Heyder, *Proc. Am. Thorac. Soc.*, 2004, **1**(4), 315–320.
62 J. W. Tang, W. P. Bahnfleth, P. M. Bluyssen, G. Buonanno, J. L. Jimenez, J. Kurnitski, Y. Li, S. Miller, C. Sekhar, L. Morawska, L. C. Marr, A. K. Melikov, W. W. Nazaroff, P. V. Nielsen, R. Tellier, P. Wargocki and S. J. Daner, *J. Hosp. Infect.*, 2021, **110**, 89–96.